Structural Characteristics and Selected Properties of Polyacrylonitrile Nanofiber Mats

Sedigheh Borhani,[1] Seyed Abdolkarim Hosseini,[1] Seyed Gholamreza Etemad,[2] Jiří Militký[3]

[1]*Department of Textile Engineering, Isfahan University of Technology, Isfahan 84156-83111, Iran*
[2]*Department of Chemical Engineering, Isfahan University of Technology, Isfahan 84156-83111, Iran*
[3]*Department of Textile Materials, Textile Faculty, Technical University of Liberec, 46117 Liberec, Czech Republic*

Received 11 June 2007; accepted 26 November 2007
DOI 10.1002/app.27904
Published online 27 February 2008 in Wiley InterScience (www.interscience.wiley.com).

ABSTRACT: In electrospinning, the structure of nanofibers, which is affected by polymer solution parameters and processing conditions, influences the physical characteristics of nanofiber mats. In this study, under optimum conditions of electrospinning, the concentration of polyacrylonitrile (PAN) was changed from 11 to 15 wt %, and its effects on the nanofiber diameter and surface porosity of nanofiber mats were studied. The results showed that increasing the PAN polymer concentration enhanced the nanofiber diameter but reduced the surface porosity of nanofiber mats. Because the diameter and surface porosity are parameters that possess mutual effects, a structural parameter (Q) was introduced, and then its relation to some of the physical characteristics, such as the air permeability and surface roughness, was investigated. To evaluate the surface roughness, atomic force microscopy (AFM) and entropy (ENT) methods were used. The surface roughness of nanofiber mats was measured by AFM in a surface noncontact mode and by ENT with an image analysis technique and co-occurrence matrix. The correlation coefficient of the surface roughness obtained from these two methods was 94%. The results also present a strong dependence between Q and the surface roughness and air permeability of nanofiber mats. © 2008 Wiley Periodicals, Inc. J Appl Polym Sci 108: 2994–3000, 2008

Key words: atomic force microscopy (AFM); fibers; nanolayers

INTRODUCTION

Fibrous materials used for filter media provide advantages of higher filtration efficiency and lower air resistance, which are closely associated with fiber fineness.[1,2] Filtration efficiency is one of the most important concerns for filter performance.[3–9] There are various methods used to produce ultrafine fibers.[1,2] Recently, much attention has been directed toward electrospinning as a unique technique for the fabrication of nanofibers.[1–13] In electrospinning, a high voltage is applied to a capillary containing a polymer solution. At a voltage sufficient to overcome surface tension forces, a charged fluid jet is ejected from the needle tip. The jet is stretched and elongated before it reaches the target and then dried and collected as randomly oriented structures in the form of a nonwoven mat.

Nanofiber is a broad term that generally refers to a fiber with a diameter less than 1 μm.[4,5] Nanofibers, because of their unique properties, such as a small diameter, a high specific surface area, and the potential to incorporate active chemistry, have many applications.[1,2]

Electrospun nanofiber mats can be produced with a wide range of porosity values. These nanowebs have good aerosol particle obstruction and comparatively low air resistance. Because of these properties, nanofiber mats are unique candidates for filtration and protective clothing. Recently, the filtration properties of electrospun mats have been studied.[3–11] To provide appropriate mechanical properties, nanofiber webs have been applied to various substrates. Substrates are often chosen to resemble conventional filter materials.[10]

Gibson et al.[6,7] reported some properties of electrospun mats. They compared performances of electrospun fiber mats with properties of textiles and membranes currently used in protective clothing systems and showed that electrospun layers are extremely efficient for trapping airborne particles. Also, they reported that the air flow resistance and aerosol filtration properties correlate with the electrospun coating add-on weight. They showed that an extremely thin layer of electrospun nanofibers eliminated particle penetration through the layer. Transport properties of electrospun nylon 6 mats were investigated by Ryu et al.[12] They found that

Correspondence to: S. A. Hoseini (hoseinir@cc.iut.ac.ir).
Contract grant sponsor: Center of Excellence for Environmental Nanotechnology and Research Center of Fiber Science and Technology, Isfahan University of Technology (Isfahan, Iran).

Journal of Applied Polymer Science, Vol. 108, 2994–3000 (2008)

the polymer solution concentration affected the fiber diameter, pore size, Brunauer–Emmett–Teller surface area, and gas transport properties of mats. It has been shown that the filtration efficiency of nylon 6 nanofilters is superior to that of a commercialized high-efficiency particulate air filter for 0.3-μm test particles.[3] Li et al.[13] found that the pore size and pore size distribution of electrospun poly(lactic acid) membranes are strongly associated with the fiber mass, fiber diameter, and fiber length.

The main aim of this study was to investigate the effect of the polyacrylonitrile (PAN) polymer concentration on the characteristics of nanofiber mats. First, the PAN polymer concentration was changed; the solution viscosity and fiber diameter were measured. The distribution of the fiber diameter was identified. Then, textural features of the mats were quantitatively evaluated. For the characterization of the mat structure, the product of the mean coverage and fiber diameter was used. Finally, the correlation between the structural characteristics of the mats and other properties of the nanofiber mats, such as the roughness and air permeability, were investigated.

Structural characteristics of nanofibrous mats

A summary of the structural models of nanofibrous assemblies (mats) and theoretical expressions for the computation of the basic structural characteristics of these assemblies is presented ref. 14. The basic relations are here adopted to compute relations between the nanofiber diameter, roughness, and porosity or pore size from basic characteristics of a nanofibrous network. This network is used as a working model for nanofibrous mats.

Nanofibers in a network are simply assumed to be solid, straight rods having length L (usually greater than 10 mm), diameter d, and linear density J, which is defined as follows:

$$J = \frac{\pi d^2 \rho}{4} \tag{1}$$

where ρ is the (volumetric) density of the fiber. The network is characterized by the porosity, which is defined usually as follows:

$$\text{Porosity} = 1 - \frac{\rho h}{w} \tag{2}$$

where h is the network thickness and w is the network areal density. In this simplified network, the locations of nanofiber centers follow a Poisson process in two dimensions, and they are independent of each other. The orientation distribution of a nanofiber to a selected direction in this random structure is described by a uniform distribution (for details, see ref. 14). The mean coverage of this network can be expressed by the following relation:

$$\text{Mean coverage} = \frac{wd}{J} \tag{3}$$

The probability that a point in this network has coverage zero is given by the Poisson distribution with the mean coverage. Under these assumptions, the porosity is related to the mean coverage as follows:

$$P_0 = \exp(-C_0) \tag{4}$$

where P_0 is the porosity and C_0 is the mean coverage.

The air permeability is dependent on the coefficient of the pressure loss and porosity. The empirical relation between the air permeability and planar weight of the fabric (w) is as follows:

$$\text{Air permeability} \approx \frac{K_1}{w} + K_2 \approx \frac{4K_1}{C_0 \pi d} + K_2 \approx \frac{4K_1}{\log(1/P_0)\pi d} + K_2 \tag{5}$$

where constants K_1 and K_2 depend on the density of the fibers and their resistance.[15] The standard deviation of the local coverage on scale x [$s(x)$] can be approximately expressed by the following relation:

$$s(x) \approx \sqrt{\left(\frac{0.95\, d\, C_0}{x}\right)} \approx k\sqrt{d\, C_0} \approx k\sqrt{\frac{4\, w}{\pi\, \rho}} \approx k\sqrt{d\, \log(1/P_0)} \tag{6}$$

where k is a constant dependent on the scale of the resolution (a scale of 1 mm corresponds to the variability detected by the human eye).

The expression of $d \log(1/P_0)$ in these equations is defined as a product of structural parameter Q.

EXPERIMENTAL

Materials

Polyacrylonitrile (PAN) with a weight-average molecular weight of about 100,000 g/mol was received from Polyacryl Co. (Isfahan, Iran). Dimethylformamide (DMF) was acquired from Merck Co. (Germany) as a solvent.

Electrospinning

Polymer solutions with concentrations of 11, 12, 13, 14, and 15 wt % were prepared by the dissolution of PAN in DMF.

The experimental setup for electrospinning is shown in Figure 1. A PAN solution in DMF was loaded into a 1-mL syringe. The polymer solution was fed at a speed of 2.8 μL/min through a needle

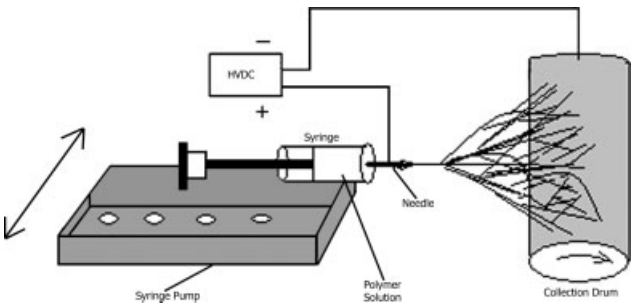

Figure 1 Schematic illustration of the electrospinning setup. HVDC, high voltage direct current source.

with an outer diameter of 0.7 mm. A 10-kV voltage was applied between the needle and a metallic collector. The tip-to-collector distance was 15 cm. To make nanofiber mats, the collector was rotated, the pump had a traverse movement, and the collector was covered with activated carbon filter media. The velocity of the collector rotation and traverse of the pump were fixed at 96 rpm and 28 mm/min, respectively. Electrospun PAN nanofibers were sprayed directly onto activated carbon filter media for an equal time of electrospinning for all solutions.

Measurements

The viscosity of the polymer solution was determined with a rheometer (RV 12, Haake, Mess-Technik GmbH, Karlsruhe, Germany) at 25°C. The morphology of the electrospun mats was observed with a Philips XL-30 scanning electron microscope (Netherlands) and a DME atomic force microscope (Denmark) with a Dual Scope DF 95-50 scanner and a Dual Scope C-21 controller. Scanning was carried out in a noncontact mode. Matic image processing software was used to calculate the diameter of PAN nanofibers from scanning electron microscopy (SEM) images at a magnification of 5000×. At least 100 fibers were used to calculate the mean values of the fiber diameter.

The distribution of the fiber diameter was evaluated with a program created in MATLAB 7. The air permeability of activated carbon filter media coated with PAN nanofibers was measured with a permeation analyzer (L-14, Karl Schroeder Co., Germany) at 25°C and 2 mbar.

With image analysis, a program was written in MATLAB to determine the surface porosity of activated carbon filter media coated with PAN nanofibers. With SEM micrographs at a magnification of 5000×, the mean values of 15 measurements were obtained.

To measure the roughness of the mats, the entropy (ENT) algorithm was used. The variations in the gray levels for images of nanofiber mats depend on the fiber diameter. Many statistical parameters are derived from collecting and adding various quantities related to the distribution of gray levels of images. The co-occurrence features are obtained as second-order statistics for image information. The co-occurrence matrix $[M(d,\theta)]$ consists of probability $p_\delta(i,j)$ ($i = 1, 2, \ldots n$), in which the pixel of gray level i appears separated by a distance of $\delta = (d,\theta)$ from the pixel of gray level j, where the parameters d and θ are the distance and positional angle between a certain gray level pair, respectively. $M(d,\theta)$ in four directions (0, 45, 90, and 135°) was determined.[16,17] ENT, based on $M(d,\theta)$, was used in this study:

$$\mathrm{ENT} = -\sum_{i=0}^{n-1}\sum_{j=0}^{n-1}\left(\frac{p_\delta(i,j)}{R}\right).\log\left(\frac{p_\delta(i,j)}{R}\right) \qquad (7)$$

where $i = 0, 1, \ldots n - 1$; $j = 0, 1, \ldots n - 1$; and R is the sum of values of $M(d,\theta)$.

Software was developed to measure the ENT of samples calculated from SEM micrographs of nanofibers placed on pores of open-cell activated carbon filter media at a magnification of 200×. Twenty repeats of measurements were realized, and the mean values were calculated.

Also, for the analysis of the surface and roughness characteristics of nanofiber mats by atomic force microscopy (AFM) images, DME SPM software was used.

A one-way analysis of variance at the 0.05 level of significance and Duncan's multiple-range test were conducted to investigate multiple comparisons among the treatments. Also, a linear regression was used to determine the appropriate correlation between variables.

RESULTS AND DISCUSSION

Nanofibers and structural parameters

The most effective parameter for controlling the fiber diameter is the solution concentration.[1,2]

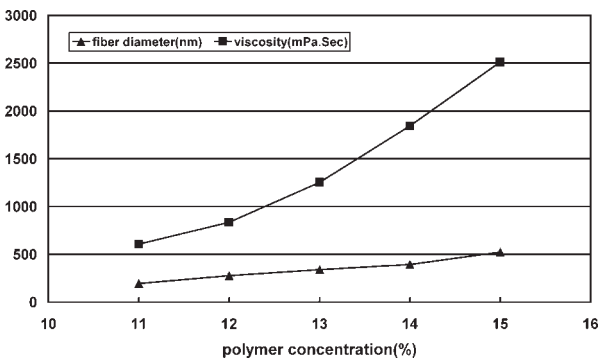

Figure 2 Effect of the PAN solution concentration on the solution viscosity and nanofiber diameter.

TABLE I
Effect of the Polymer Solution Concentration on the Surface Properties of Nanofiber Mats

Polymer concentration (%)	Polymer viscosity (mPa s)	Nanofiber diameter (nm)	Surface porosity (%)	Air permeability (L/m^2 s)	AGR (nm)	ENT
11	608.6	195.1 ± 42.03	81.4 ± 4.5	2700 ± 0	66.42	1.06 ± 0.12
12	836.8	277.5 ± 39.94	78.8 ± 4.6	2700 ± 100	152.09	1.1 ± 0.23
13	1252.4	340.55 ± 54.5	80.8 ± 4.2	2400 ± 0	276.93	1.37 ± 0.25
14	1845.1	394.67 ± 52.76	72.4 ± 7.8	2200 ± 100	332.22	1.34 ± 0.23
15	2512.7	523.94 ± 116.85	73.4 ± 8.7	2267 ± 152.8	404.44	1.43 ± 0.27

In ref. 18, the description of the dependence of the fiber diameter (d) on the PAN/DMF solution concentration (C) in the range of 6–12 wt % is approximated by the following relation:

$$d = 2241.77 - 575.57\,C + 40.25\,C^2 \quad (8)$$

Figure 2 and Table I present the effects of the PAN solution concentration on the surface properties of nanofiber mats. The results indicate an increase in the polymer viscosity with an increase in the PAN polymer concentration. Because a higher viscosity leads to greater resistance of the solution, the diameter of the fiber increases. The average enhancement of the fiber diameter was found to be 195 ± 42 to 524 ± 116 nm when the solution concentration was changed from 11 to 15 wt %.

The program created in MATLAB 7 was used for selection between normal, lognormal, and Weibull distributions and for the evaluation of corresponding parameters. In all cases, the three-parameter Weibull distribution was evaluated to be the best one. Typical results for a polymer concentration of 15 wt % are shown in Figure 3. The median values computed from this distribution are given in Table II. These robust estimates of the fiber diameter were used for the computation of the mean coverage from eq. (4) and the Q product (Q = mean coverage × fiber diameter). These characteristics are given in Table II.

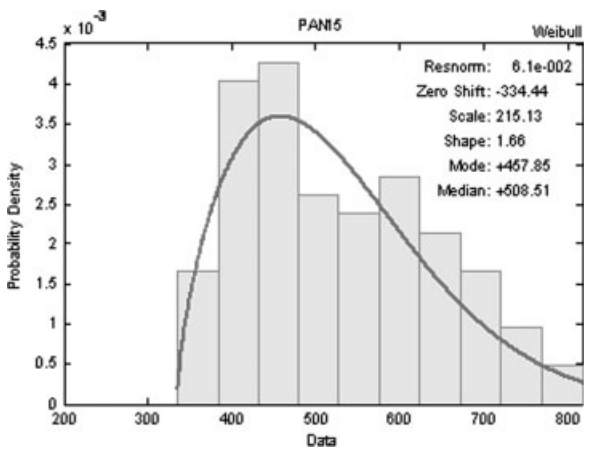

Figure 3 Distribution of the fiber diameter for a polymer concentration of 15 wt %.

Surface porosity and air permeability

Typical SEM micrographs of PAN nanofibers at different concentrations are shown in Figure 4. These micrographs provide visual confirmation of the difference in both the fiber diameter and surface porosity between samples. On the basis of the results of Table I, the surface porosity of the samples decreased with an increase in the fiber diameter. Statistical analysis showed that the surface porosity significantly decreased as the fiber diameter increased. The noticeable reduction in the air permeability of samples was also found with increasing fiber diameter. From eq. (5), it has been determined that the air permeability is a linear function of $1/Q$. The relationship between the air permeability and $1/Q$ is shown in Figure 5. The results indicate that there was a linear relation between $1/Q$ and the air permeability of the samples, and a correlation coefficient of about 0.86 was obtained.

ENT

As mentioned before, according to statistics and theoretical information, ENT is a measure of the surface roughness or complexity.[16]

Typical SEM micrographs of nanofibers placed on pores of open-cell activated carbon filter media are shown in Figure 6. ENT was obtained from the co-occurrence matrix for the directions of $\theta = 0$, 45, 90, and 135° for $d = 1$, and the mean values for these directions were computed. The results are presented in Table I. Figure 7 illustrates the effect of the nanofiber diameter on ENT of filter media. The results reveal that ENT tends to increase with increasing fiber diameter. In other words, increasing the nano-

TABLE II
Computed Structural Characteristics of the Nanofiber Mats

Polymer concentration (%)	Fiber diameter median (nm)	Mean coverage (—)	Product Q (nm)
11	189.76	0.206	39.05
12	270.80	0.238	64.52
13	342.18	0.213	72.95
14	388.46	0.323	125.46
15	508.51	0.309	157.25

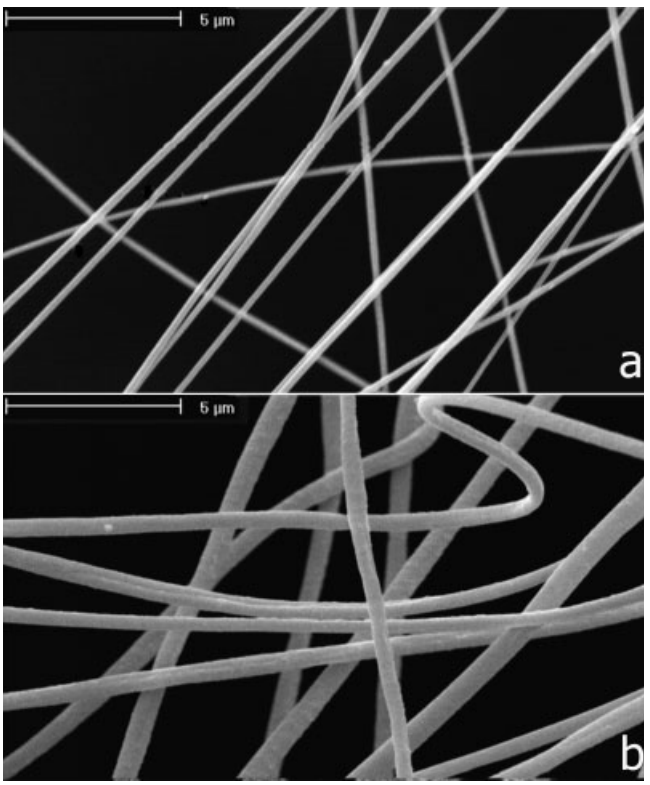

Figure 4 SEM micrographs of PAN nanofibers at different concentrations: (a) 11 and (b) 15 wt %.

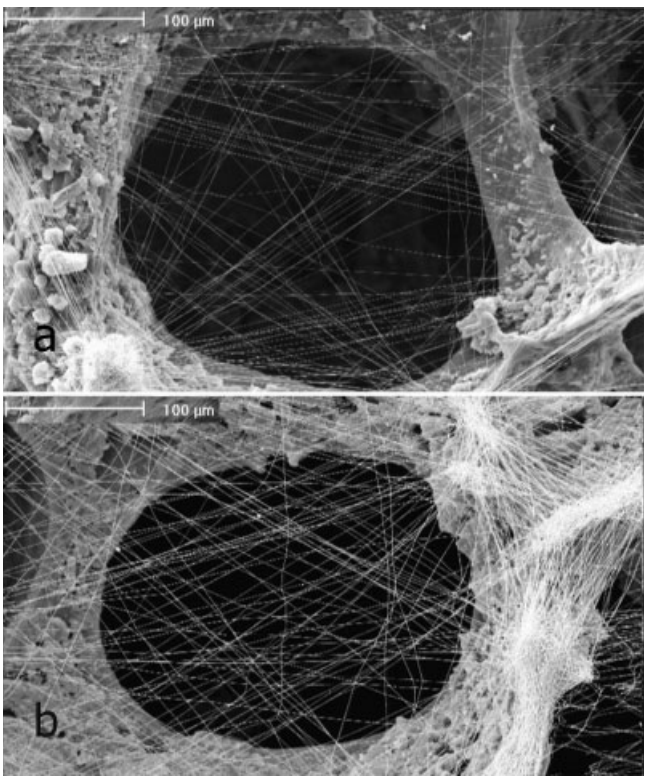

Figure 6 SEM micrographs of PAN nanofibers: (a) 11 and (b) 15 wt %.

fiber diameter enhances the surface roughness of nanofiber mats, and here a correlation coefficient of about 0.90 was obtained.

AFM

AFM produces topographical images by scanning a sharp tip, situated at the end of a microscopic cantilever, over a surface. The technique has been used to produce images of many materials, and the resolution can reach atomic dimensions for flat surfaces. AFM can give useful information about surface morphology.[19,20] Figure 8(a–e) shows typical three-dimensional (3D) AFM images of each of the mats over an area of 10 µm × 10 µm. The color intensity shows the vertical profile of the mat surface. The light regions are related to the highest points, and the dark regions are related to pores and valleys. Table I reports that the average geometric roughness (AGR) is equal to the standard deviation of heights for the images of Figure 8. The mean values and

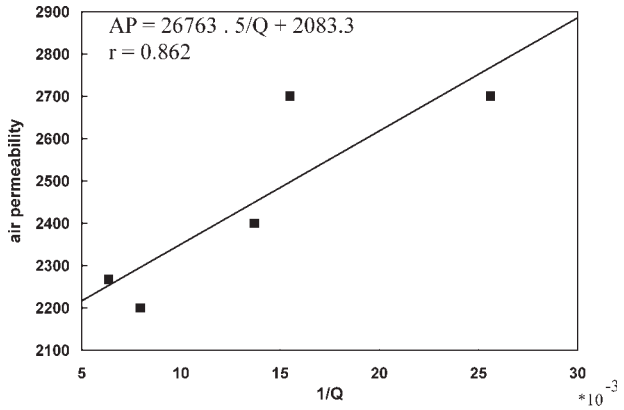

Figure 5 Relation between the air permeability (AP) and $1/Q$ [see eq. (5)].

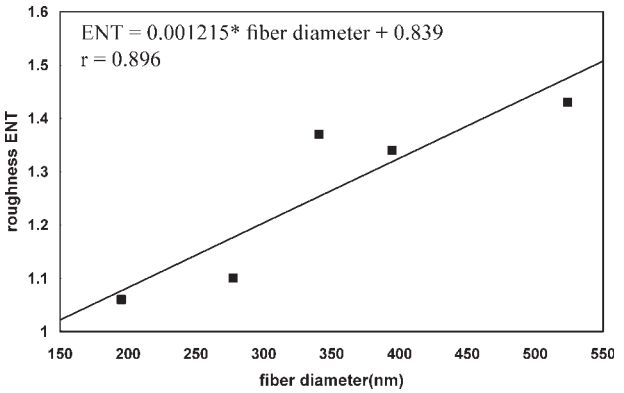

Figure 7 Relation between the nanofiber diameter and ENT of filter media.

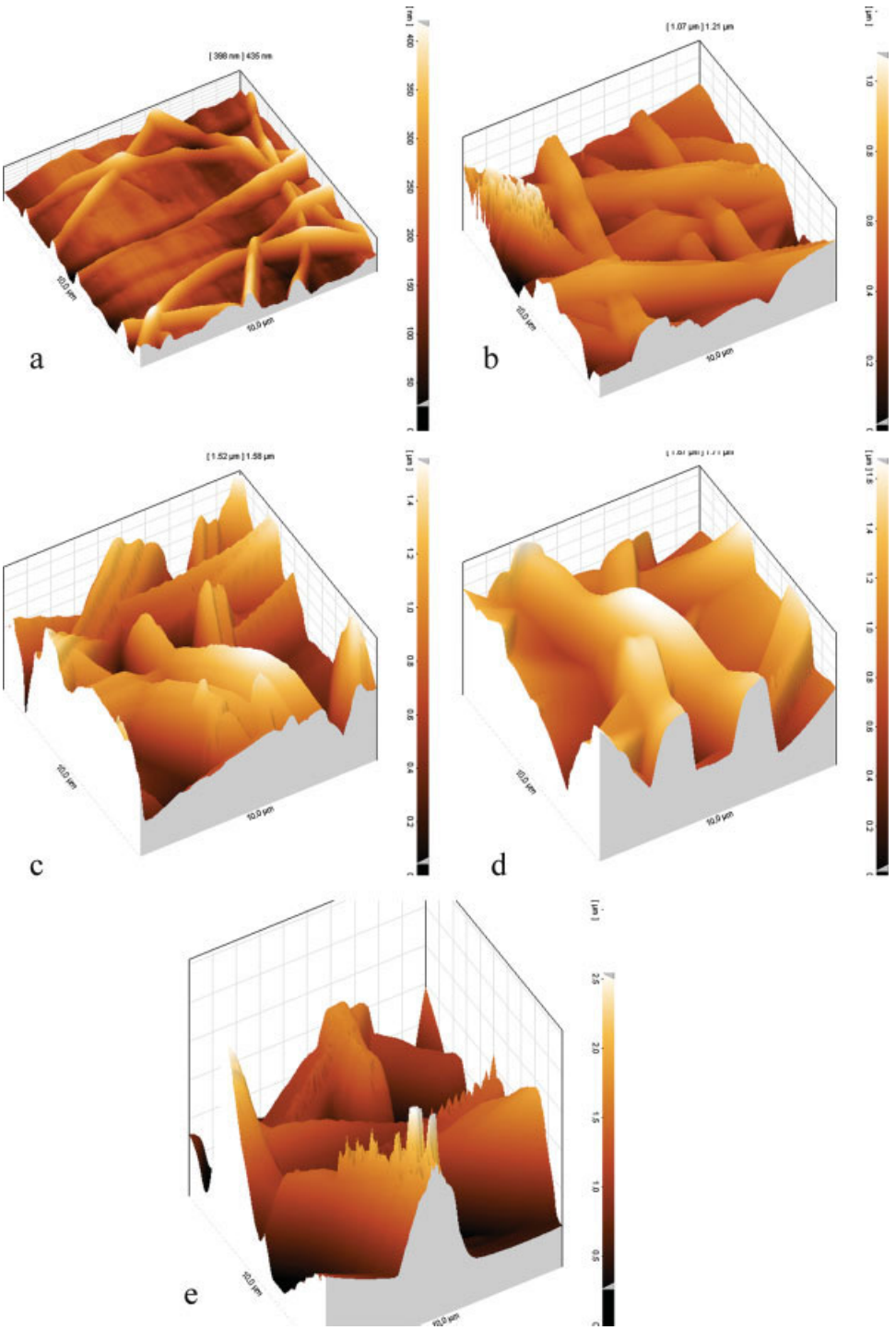

Figure 8 3D AFM micrographs of PAN nanofiber mats: (a) 11, (b) 12, (c) 13, (d) 14, and (e) 15 wt %. [Color figure can be viewed in the online issue, which is available at www.interscience.wiley.com.]

standard deviations reported were obtained by the division of each 10 μm × 10 μm area into nine equal square regions and the subsequent assessment of the roughness of each region. On the basis of the results of Figure 8 and Table I, the finest fibers and smoothest surface belonged to a polymer solution with an 11 wt % concentration, whereas the coarsest fibers and roughest surface belonged to the sample with a 15 wt % PAN solution. The relationship between AGR and the square root of the product [sqrt(Q)] is shown in Figure 9. AGR is a linear function of sqrt(Q). The correlation coefficient is about 0.96. In fact, $s(x)$ from eq. (6) is directly connected to AGR evaluated from AFM images.

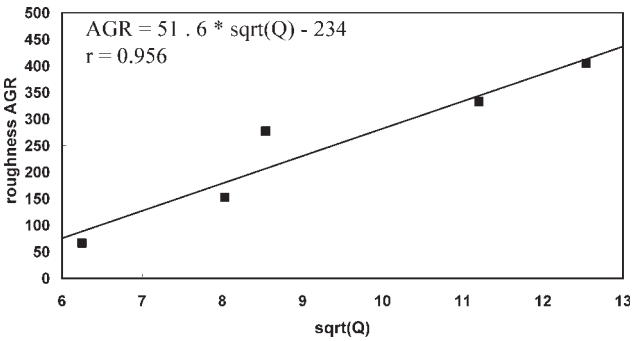

Figure 9 Relation between AGR and sqrt(Q) [see eq. (6)].

It is interesting that AGR and air permeability are functions of $Q = d \log(1/P_0)$.

CONCLUSIONS

The structural parameter Q is a suitable composite measure of the structure of mats. In this study, new techniques for assessing the surface roughness of nanofiber mats were employed. To analyze the variations of the surface roughness quantitatively, ENT of the co-occurrence matrix and AGR of AFM images were obtained. Experimental results indicated the existence of a good correlation between Q (a function of the fiber diameter and surface porosity) and the air permeability or surface roughness of nanofiber mats. This investigation shows that approximate theoretical equations derived from a model of mats as a random network composed of straight fibers is able to predict the form of dependences between structural characteristics and roughness or air permeability. Corresponding correlation coefficients are high. Also, there was a linear relationship between the results of the ENT algorithm and AFM method with a correlation coefficient of 0.94.

References

1. Huang, Z. M.; Zhang, Y. Z.; Kotaki, M.; Ramakrishna, S. Compos Sci Technol 2003, 63, 2223.
2. Ramakrishna, S.; Fujihara, K.; Teo, W. E.; Lim, T. C.; Ma, Z. In An Introduction to Electrospinning and Nanofibres; World Scientific, 2005.
3. Ahn, Y. C.; Park, S. K.; Kim, G. T.; Hwang, Y. J.; Lee, C. G.; Shin, H. S.; Lee, J. K. Curr Appl Phys 2006, 6, 1030.
4. Kosmide, K.; Scott, J. http://www.filtsep.com, July/August 2002, 20.
5. Graham, K.; Ouyang, M.; Raether, T.; Grafe, T.; McDonald, B.; Knauf, P. Presented at the 15th Annual Technical Conference & Expo of the American Filtration & Separations Society, Galveston, TX, April 9–12, 2002.
6. Gibson, P.; Gibson, H. S.; Rivin, D. Colloids Surf A 2001, 187, 469.
7. Gibson, P.; Gibson, H. S.; Rivin, D. AIChE J 1999, 45, 190.
8. Gopal, R.; Kaur, S.; Feng, C. Y.; Chand, C.; Ramakrishna, S.; Tabe, S.; Matsuura, T. J Membr Sci 2007, 289, 210.
9. Barhate, R. S.; Loong, C. K.; Ramakrishna, S. J Membr Sci 2005, 283, 209.
10. Grafe, T.; Going, M.; Barris, M.; Schaefer, J.; Canepa, R. Presented at the International Conference and Exposition of the INDA; Chicago, Illinois, Dec 3–5, 2001.
11. Yoon, K.; Kim, K.; Wang, X.; Fang, D.; Hsiao, B. S.; Chu, B. Polymer 2006, 47, 2434.
12. Ryu, Y. J.; Kim, H. Y.; Lee, H. K.; Park, H. C.; Lee, D. R. Eur Polym J 2003, 39, 1883.
13. Li, D.; Frey, M. W.; Joo, Y. L. J Membr Sci 2006, 286, 104.
14. Eichhorn, J.; Sampson, W. W. J R Soc Interface 2005, 2, 309.
15. Militky, J. Proc Natl Conf Text Eng, May 8–10, 2007, 3.
16. Mohri, M.; Hosseini Ravandi, S. A.; Youssefi, M. Text Inst 2005, 96, 365.
17. Haralick, R. M.; Shanamugam, K.; Dinstein, I. IEEE Trans Syst Man Cybern 1973, 3, 610.
18. Gu, S. Y.; Ren, J.; Vansco, G. J. Eur Polym J 2005, 41, 2559.
19. Zolfaghari, A.; Almasi, M.; Marashi, P.; Najba, M.; Seifi, O. Scanning Probe Microscopy: The Lab on a Tip; Peyke Noor: Tehran, 2007.
20. Bowen, W. R.; Doneva, T. A. Desalination 2000, 129, 163.